Wolfgang Lubitz, Thomas Lohmiller and Nicholas Cox

WATER OXIDATION AND OXYGEN EVOLUTION IN PHOTOSYNTHESIS. AN ENZYME THAT CHANGED THE WORLD

INTRODUCTION

The evolution of an enzyme that was able to split water into molecular oxygen and bound hydrogen was a unique event in the development of our planet and higher life on earth. This process first developed by simple cyanobacteria and later used in identical form by other photosynthetic organisms from unicellular algae to higher plants enabled these species to efficiently reduce CO_2 to carbohydrates, using the abundant water as convenient electron source. Via photosynthesis, the energy of the sun is stored in energy-rich compounds, which represents the central metabolic pathway to supply our biosphere with energy and biomass. In this process, water splitting leads to the release of O_2 as waste product. Starting more than 2.5 billion years ago, this led to the formation of the oxygen-rich atmosphere of our planet. This great oxygenation event was a catastrophe for most simple life forms that had no defense mechanism to cope with the toxic oxygen and thus died and finally disappeared. But at the same time, the presence of O_2 in the atmosphere stimulated the development of higher, aerobic life forms on earth, i.e. organisms that learned to use oxygen for their metabolism. Without the earlier invention of oxygenic photosynthesis, this development of complex life forms with cellular respiration including human beings would not have been possible. It is therefore not only of scientific but also of cultural value for mankind to understand how water oxidation and oxygen release function in natural photosynthesis.

Mankind benefits from photosynthesis in many ways. The products of this largest chemical process on earth are the only source of food and thus cover our entire energy demand. Furthermore, it supplies us with valuable natural materials like wood, paper, cotton, peat and biomass in general. Plants also contain many important bioactive materials that are used as drugs, in cosmetics, as natural dyes etc. Last but not least, photosynthesis is also the source of all fossil fuels oil, coal and natural gas. It can thus be considered the basis of our life on earth.

Prof. Dr. Wolfgang Lubitz, Dr. Thomas Lohmiller and Dr. Nicholas Cox
Max-Planck-Institut für Chemische Energiekonversion, Mülheim/Ruhr
Research School of Chemistry, Australian National University,
Canberra, Australia (Nicholas Cox)
E-Mail: wolfgang.lubitz@cec.mpg.de
E-Mail: thomas.lohmiller@cec.mpg.de
E-Mail: nicholas.cox@cec.mpg.de

Over the last 150 years, we have massively used fossil fuels to cover the ever-increasing energy demand of our human society,[1] which accompanied the industrial revolution in the 19th and 20th century. The strong rise in energy consumption in the developed and emerging countries has led to a shortage of these resources, with the economic, social and political consequences already felt today. Scientists agree[2] that the burning of carbon-rich fossil fuels has contributed very significantly to the increase of CO_2 concentrations in the atmosphere and the associated anthropogenic climate changes with severe effects for our planet and human life. It is therefore one of the great challenges of our time to identify and develop alternative sustainable energy resources.[3-6]

A basic understanding of the ways how nature stores energy and in particular uses sunlight to split water could show us future ways to harvest and store the sun s abundant energy to satisfy the energy demand of mankind in the future. However, this requires a global effort in the field of artificial photosynthesis .[7-9] In the present article, the current knowledge of the principles of photosynthetic water oxidation are described, which is considered one of the holy grails of chemistry.

LIGHT HARVESTING AND CHARGE SEPARATION IN OXYGENIC PHOTOSYNTHESIS

In oxygenic photosynthesis of plants, algae and cyanobacteria, sunlight is collected by the light harvesting complexes (LHCs), specialized chlorophyll (and carotenoid) containing proteins, which show a large variation depending on the type of organism.[10] The light energy is funneled to a reaction center (RC) where charge separation across the photosynthetic membrane takes place. In oxygenic photosynthesis, two RCs photosystem (PS) I and II work in tandem to create the enormous redox span necessary to drive the coupled reactions. This process provides electrons with sufficiently negative potential needed to reduce $NADP^+$ to NADPH, which can be considered bound biological hydrogen . The electrons for this process originate from water oxidation that takes place in PS II. The water splitting and subsequent reactions also generate a proton gradient across the photosynthetic membrane, which is used by the enzyme ATPase to produce ATP, nature s main energy currency, from ADP. In a different cell compartment, ATP and NADPH are then used to reduce CO_2 to carbohydrates in the so-called dark reactions (Calvin-Benson Cycle).[11]

Fig. 1 shows the dimeric PS II protein,[12] located in the photosynthetic membrane. Each monomer is made up of 19 protein subunits. A few important ones are indicated in the figure, including: CP43 and CP47, which bind the core antenna pigments; D1 and D2, which bind all pigments of the reaction center and all cofactors of the electron transport chain; and the small subunits PsbO, PsbU and PsbV, which stabilize the water splitting cofactor. Below, the cofactor arrangement in D1/D2 is shown comprising chlorophylls (P_{D1}, P_{D2}, Chl_{D1}, Chl_{D2}, $Chlz_{D1}$, $Chlz_{D2}$), carotenoids (Car_{D1}, Car_{D2}), two pheophytins ($Pheo_{D1}$, $Pheo_{D2}$), two plastoquinones (Q_A, Q_B), one non-heme iron (Fe) and also the water oxidizing complex (WOC), a Mn_4O_xCa cluster (see Fig. 2, top). This cubane-like cluster comprises four Mn and one Ca ion linked by five to six oxygen bridges, depending on the state in the water splitting cycle. Remarkably, it also binds two water molecules, two at the Ca (W3 and W4) and two at the dangling Mn_A (W1 and W2). The cluster is connected to the protein surface via specific channels for the efficient uptake of water and the release of protons and of molecular oxygen.

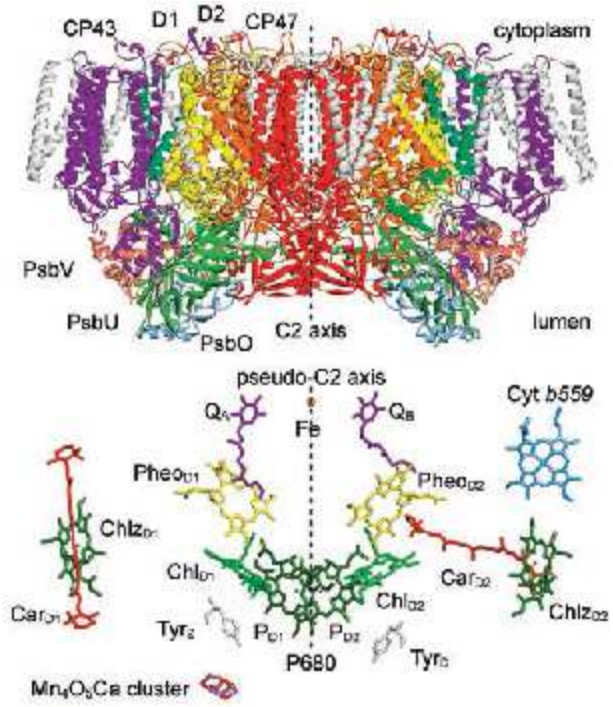

Fig. 1: Top: X-ray crystallographic structure of photosystem II (PS II) from *Thermosynechococcus vulcanus*[12] showing the dimeric character of the protein (molecular weight of the dimer: ≈700 kDa); the two monomers are related to each other by a C2 axis. The most important subunits are indicated, with the D1 protein in yellow carrying the cofactors and the Mn cluster. Bottom: Pigment arrangement in one monomer (two branches related by a pseudo-C2 axis) showing the primary donor P680 (four chlorophylls: P_{D1}, P_{D2}, Chl_{D1}, Chl_{D2}), the electron acceptors pheophytin (Pheo), plastoquinones (Q_A, Q_B), and the non-heme iron Fe. Additional chlorophylls (Chlz) and carotenoids (Car), as well as two redox active tyrosines (Y_Z, Y_D) are also indicated. Next to the active branch (D1) and close to Y_Z/P680, the manganese cluster Mn_4O_5Ca is located. For further details see refs. [12-13].

In the D1 protein, light-induced charge separation takes place, transporting electrons across the membrane to the quinones and leaving behind the cation radical of the primary donor, $P680^{\bullet+}$, a chlorophyll assembly that has a very high oxidizing power (> +1.2 eV). It is important to note that the high potential is needed for water oxidation, but is also dangerous since this radical cation can, in principle, oxidize neighboring chlorophylls, certain amino acids, and even water molecules. To diminish such side reactions, nature has placed a redox active tyrosine residue (Tyr_Z or Y_Z) next to $P680^{\bullet+}$ that is able to quickly donate an electron to this species on a nanosecond time scale; thereby reducing the radical cation to its initial state P680. $Y_Z^{\bullet+}$ is stabilized by losing a proton to a neighboring histidine in a reversible fashion, forming a neutral radical ($Y_Z^{\bullet}$). $Y_Z^{\bullet}$ in turn oxidizes the adjacent Mn cluster. It thus acts as a highly efficient interface between the fast charge separation in PS II and the slow water splitting process at the Mn cluster,[15] and at the same time serves to diminish damage in PS II.

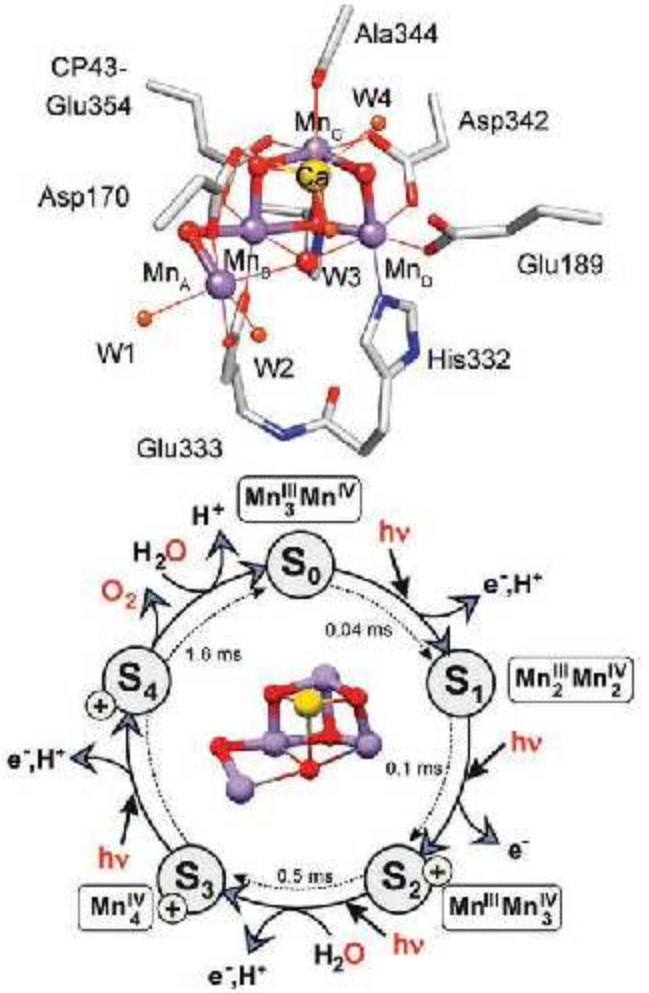

Fig. 2: Top: Structure of the water oxidizing Mn_4O_5Ca cluster in PS II[12] with 4 Mn ions (Mn_A to Mn_D) and Ca, bridged by oxygen ligands. Three Mn ions, the Ca and their bridging oxygen ligands form a distorted cube, the fourth Mn (Mn_A) is dangling. Mn_A and the Ca carry two water molecules each. The coordination of the metal ions by amino acid ligands is also shown. Bottom: Water oxidation cycle (Kok cycle)[14] showing the five basic S states (S_0 to S_4), the Mn oxidation states, the light-induced $1e^-$ oxidation steps, the proton release pattern and the substrate water uptake, besides the reaction times for the single electron oxidation steps. Note that here, the S stands for state, not for the electron spin.

However, another light-induced process that occurs in PS II is even more dangerous, for which nature has not found a perfect solution to prevent it. This is the creation of triplet states, e.g. of the chlorophylls in the core antenna via intersystem crossing or in the RC via (triplet) radical pair recombination. While carotenoid molecules are present in PS II to suppress (quench) triplet chlorophyll formation, these states can still react with

triplet oxygen ($^3O_2$) formed in the water oxidation process yielding singlet oxygen ($^1O_2$). This very aggressive species can react with the pigments and the protein, resulting in damage of the D1 protein subunit of the PSII supercomplex, which thus has a mean life time of only 30 minutes under normal light conditions. Nevertheless, with a remarkable efficiency (2 ms turnover time), it performs about 10^6 reaction cycles before it must be replaced. Fortunately, the organisms performing oxygenic photosynthesis have developed an efficient repair mechanism for the PS II supercomplex by replacement of the D1 protein.[16]

In summary, PS II is a water:plastoquinone oxidoreductase.[17] The products are molecular oxygen (O_2), protons and reduced plastohydroquinone that are deliberated. The light-induced process in PS II is very efficient, with a quantum yield of over 90% and an energy efficiency of about 20%.

STRUCTURE AND BASIC FUNCTION OF THE WATER OXIDIZING COMPLEX IN PS II

The geometric structure of the Mn cluster has only become available recently due to the X-ray crystallographic work of Jian-Ren Shen and colleagues (see refs. [12-13]). Earlier structures[18-20] suffered from radiation damage that caused a reduction of the Mn ions in the intense X-ray beam that leads to (partial) disintegration of the complex,[21] blurring the electron density of the cluster. The recent structures of the Mn_4O_5Ca cluster avoid this problem, accurately resolving all its direct amino acid ligands (Fig. 2, top). In collaboration with colleagues at our institute, we have investigated the cluster using theoretical (DFT) methods,[22] also evaluating the protonation of the cluster in great detail.[23] This work showed that in particular the position of one of the oxygen bridges, O5, had to be corrected with respect to the X-ray structure. Interestingly, during certain states of the catalytic cycle, O5 can take two positions of almost equal energy, which changes the precise electronic properties of the cofactor. These two forms are termed the open cubane and closed cubane structures (Fig. 3). The investigation of the protonation states showed that one of the water ligands bound to Mn_A is deprotonated (OH^-).

It was discovered by Pierre Joliot almost half a century ago[25] that PS II releases oxygen after four consecutive light flashes. This shows that four light-induced trans-membrane charge separation events are necessary before one O_2 molecule is formed and released. The result is in complete agreement with the fact that the oxidation of two water molecules to produce a single molecule of O_2 is a 4-electron process,

$$2\,H_2O \rightarrow O_2 + 4\,H^+ + 4e^- \qquad (1)$$

whereas the charge separation across the membrane is a 1-electron process. The oxidizing equivalents for the water oxidation reaction are stored transiently by the the tetranuclear Mn cluster, an insight that came from Bessel Kok.[14] His so-called Kok cycle (S-state cycle) of water oxidation, shown in Fig. 2 (bottom), comprises five distinct states, S_0 to S_4, which differ by the number of electron holes transiently stored in the cofactor, as indicated by their subscript. The cycle is driven by four light absorption events ($h\nu$), by which electrons are withdrawn from the metal ions and protons are released to prevent the accumulation of positive charges and thus a Coulomb explosion of the cluster. Experimental data indicates that the two substrate waters are bound at different times in the cycle[26]. O_2 is released in a concerted reaction in the last reaction step. Kinetic measurements show that the reaction times lie in the micro- to millisecond range; the complete cycle turns over in about 2 ms.

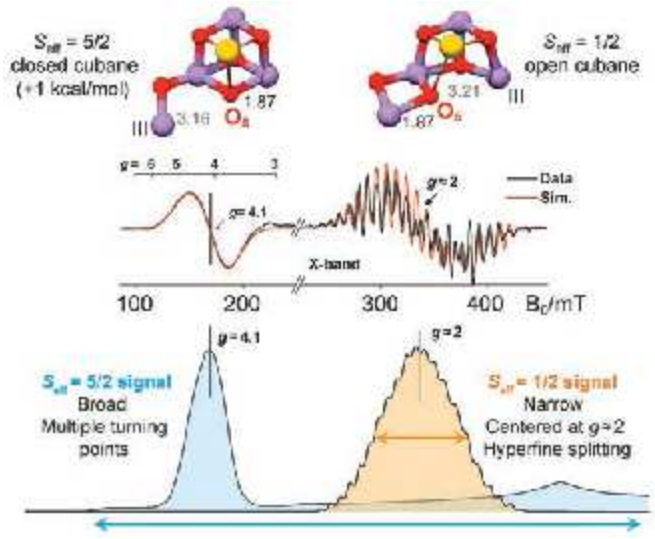

Fig. 3: DFT-optimized structures of the Mn_4O_5Ca cluster in the S_2 state. Note that the closed cubane and open cubane structures have almost the same energy but different positions of the Mn^{III} ion (Mn_A vs. Mn_D, respectively) and different total (effective) spin ground states. This explains the two EPR signals observed for this state, shown below (first derivative), around g = 4.1 (S_{eff} =5/2; no hyperfine structure) and around g = 2 (S_{eff} = ½; multiline signal). The bottom trace shows simulations of the two absorption signals. Figure adapted from refs. [22, 24].

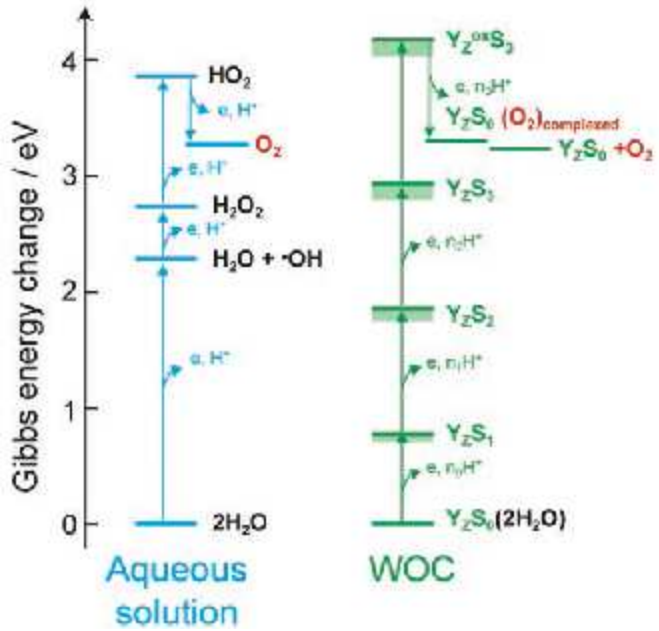

Fig. 4: Gibbs energy (in eV) required to oxidize water in aqueous solution (left) and in the WOC of PS II (right). Note that in the WOC, water is not oxidized by sequential single-electron removal from substrate water. Instead, the Mn cluster is oxidized by four successive oxidation events, the two attached substrate water molecules release the protons (for charge neutrality), and O_2 is released only in the last step after O-O bond formation in a concerted reaction. Thereby, high energy steps are avoided and the redox process is leveled. Figure adapted from ref. [27].

The reason why the Mn_4O_xCa cluster functions in this way is two-fold: (i) The energetic cost of water splitting is lowered by first storing oxidizing equivalents and then performing the 4-electron chemistry (Fig. 4); (ii) this sequence avoids the formation of reactive oxygen species (ROS) intermediates from partial oxidation of substrate water, which are highly reactive and can destroy the PS II protein complex. Instead, the Mn ions (and/or their ligands) are oxidized four times by the neighboring tyrosine $Y_Z^{\bullet}$, triggered by four charge separation events in PS II, before the cluster removes four electrons from two bound water molecules in a concerted reaction leading to O_2 release and regeneration of the original starting state of the Mn cluster. The Mn cluster thus solves the problem of how to couple the very fast light reaction (ps time scale) and the slow catalytic reaction (ms time scale) of the 4-electron water oxidation chemistry.

THE ELECTRONIC STRUCTURE OF THE Mn_4O_xCa CLUSTER

A detailed understanding of the catalytic water-oxidation reaction requires, besides the spatial structure and the kinetics and energetics of the reaction, a profound knowledge of the electronic structure, i.e. the distribution of the electrons in the cluster, in all consecutive reaction steps. The oxidation and spin states of the Mn ions, representing the total number and configuration of electrons in the Mn valence orbitals, give a simplified description thereof. Together with the magnetic interactions between the spin-bearing Mn ions, depending to a large part on the metal ligands, especially the bridging ones, they provide a comprehensive picture of the respective electronic state, which governs the chemical and catalytic properties of each S state.

An experimental method to investigate these properties is electron paramagnetic resonance (EPR) spectroscopy. It exploits a fundamental property of matter, which is that unpaired electrons have an intrinsic angular momentum (spin), which can be excited by microwave radiation in a magnetic field. The unpaired electron spin also interacts with other electron and nuclear spins as well as with local electric field gradients, making it a sensitive reporter of its chemical environment. It is thus analogous to other magnetic spectroscopies such as nuclear magnetic resonance (NMR). Since the Mn ions are open-shell species, i.e. exhibit orbitals with single electron occupancy, whereas most of the electrons of the protein and solvent surrounding are paired, the EPR signals of the Mn_4O_xCa cluster can be detected selectively. For the states S_0, S_1, S_2 and S_3, EPR experiments revealed different effective total spins S_{eff} of ½, 0, ½ (see ref. [28]) and 3 [29], which result from the specific coupling of the electron spins of the four Mn ions via super-exchange interactions. Importantly, as super-exchange mechanisms depend on how the Mn ions are connected, the spin states provide information about how the structure of the cofactor evolves during the S-state cycle. In the S_2 state, besides the low-spin S_{eff} = ½ form, showing the characteristic Mn multiline signal around g = 2,[30] the cluster can also be found in a high-spin S_{eff} = 5/2 form, as evident from the corresponding EPR signal around g = 4.1 (Fig. 3).[31-34] The two electronic structures are an immediate consequence of the different spatial conformations that have been found and characterized by DFT calculations (see above): closed cubane (S_{eff} = 5/2) and open cubane (S_{eff} = ½).[22] The effective spin S_{eff} is thus a crucial parameter for describing a particular state of the cluster and assigning it a spatial structure. For the S_3 state (Fig. 5), by measuring the Rabi oscillations via a spin nutation experiment, it was possible to unambiguously determine the effective spin S_{eff} to be 3.[29]

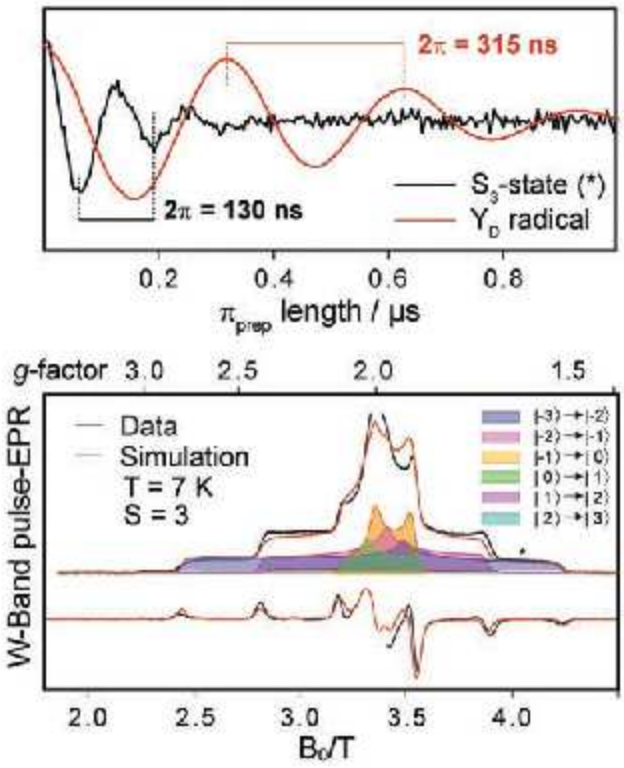

Fig. 5: W-band (94 GHz) EPR spectrum of the WOC in the S_3 state, showing an S_{eff} = 3 ground state. The spectrum is dominated by the zero-field splitting (ZFS), effective in high-spin systems. The subspectra of the different EPR multiplets with the respective ΔM_S transitions are shaded in color. On top, a spin nutation experiment is shown, performed at the high field transition $|2\rangle \rightarrow |3\rangle$ (indicated by an asterisk in the bottom panel). The nutation is compared with the corresponding experiment performed for the Y_D radical (S_{eff} = 1/2), clearly showing that the S_3 state is high spin, effectively carrying 6 unpaired electrons (S_{eff} = 3). Figure adapted from ref. [29].

Moreover, the effective electron spin of the cluster interacts with the spins of magnetic nuclei, such as ^{55}Mn, $^{1}H/^{2}H$, ^{14}N and ^{17}O. These interactions can be detected and analyzed using double resonance experiments, which are able to directly resolve nuclear spin transitions, similar to NMR experiments (see ref. [28]). ^{55}Mn electron-nuclear double resonance (ENDOR) allowed for the characterization of the S_0, S_2 and S_3 states based on electron spin coupling models. This led to the assignment of the Mn ion oxidation states, yielding $Mn^{III}_3Mn^{IV}$ for S_0,[35] $Mn^{III}Mn^{IV}_3$ for S_2,[35-37] and Mn^{IV}_4 for S_3.[29] By combination of the ^{55}Mn ENDOR results with DFT computations, oxidation states could even be assigned to the individual Mn ions, and reliable spatial models of these states be identified (Fig. 9).[24, 38] Furthermore, biochemical modifications of the Mn_4O_xCa cluster, such as the exchange of the Ca^{2+} ion for Sr^{2+} (Mn_4O_xSr) or its complete removal (Mn_4O_x), provided further insight into the conformation and number of ligands of individual Mn ions (coordination geometry) in the S_2 state (Fig. 6)[37] and information about the role of the Ca^{2+} ion. Its removal has no substantial effect on the EPR parameters of the S_2 state; the Ca^{2+} ion is thus not crucial for maintaining

its electronic structure.[39] Instead, the Ca^{2+} ion might serve as stage for the delivery of water molecules to the reaction site, affect the function of Y_Z,[15] and introduce the property of structural flexibility allowing the cofactor to toggle between the different motifs of the open and closed cubane structures. This latter property has recently been proposed as crucial for substrate binding (see below).

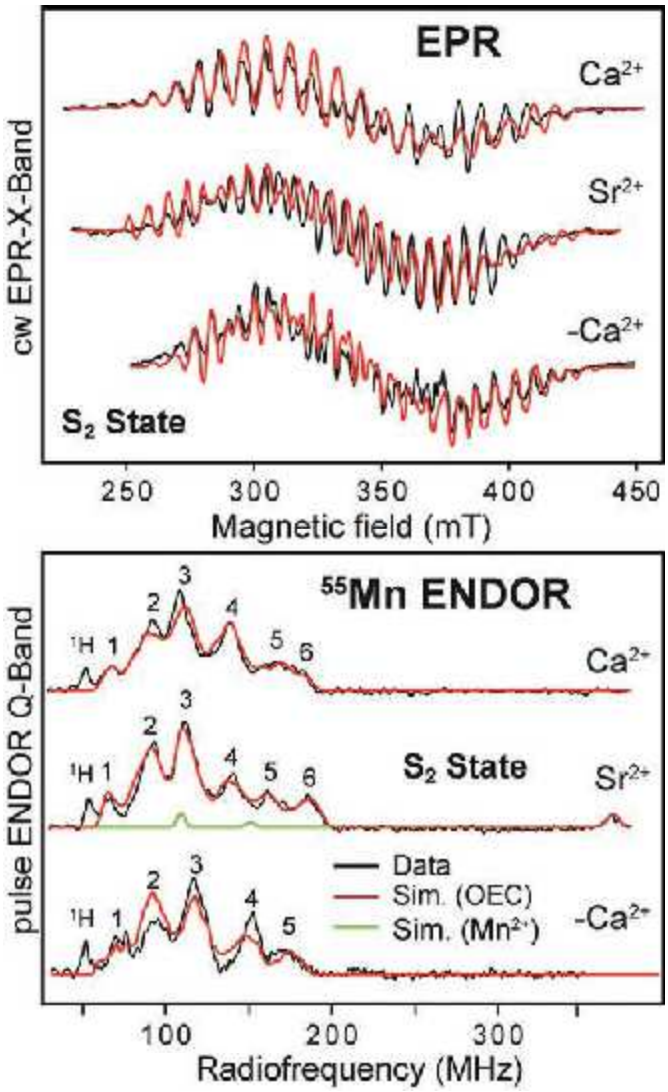

Fig 6: Multiline X-band (9 GHz) EPR (top) and Q-band (34 GHz) ^{55}Mn ENDOR (bottom) spectra for the low-spin S_2 state (g = ½, Fig. 3) of PS II samples with Ca^{2+},[37] with Sr^{2+} replacing the Ca^{2+},[37] and after Ca^{2+} removal.[39] In EPR and ENDOR, only small differences are detected for the three samples, indicating that Ca^{2+} does not significantly affect the electronic structure of the spin-coupled Mn_4 cluster.

FROM IDENTIFICATION OF THE SUBSTRATE WATER MOLECULES TO THE REACTION MECHANISM

Knowledge of the binding and dynamics of substrate water molecules is crucial for formulating the reaction mechanism of photosynthetic water oxidation. Structures from X-ray diffraction up to now have not been able to provide this information as they do not resolve the substrates in the S states directly preceding the O-O bond formation. Further candidates for substrate waters, besides the four H_2O/OH^- molecules (Fig. 2, top) directly attached to the cluster,[12, 23] are oxygen bridges within the cluster as well as possible water molecules binding at a later point in the catalytic cycle. Experimental techniques to investigate the substrates other than X-ray diffraction are EPR and vibrational (infrared) spectroscopy as well as detection of the O_2 molecules generated by time-resolved mass spectrometry (MS). The latter showed that the two substrate water molecules bind in different S states and at different sites.[26] A slowly exchanging water (W_s) binds in S_0, while a fast exchanging water (W_f) reaches its final binding site at a later stage in the cycle.

For the detection of water molecules in the WOC, EPR spectroscopy makes use of interactions with nuclear spins, preferentially ^{17}O in PS II samples with isotope-labeled $H_2{}^{17}O$ as the solvent. Methodological and instrumental developments in our laboratory allowed us to characterize the ^{17}O signals in the S_2 state using electron-electron double resonance (ELDOR)-detected NMR (EDNMR) at high frequency (94 GHz), which yields significantly better sensitivity compared with ^{17}O ENDOR (Fig. 7).[40] Through spectral simulations, we could identify the μ-oxo bridge O5 to be an exchangeable ligand in the S_2 state (Fig. 8).[40-42] Based on the following, O5 represents the most probable candidate for the twofold deprotonated substrate W_s: (i) It is the only exchangeable ^{17}O nucleus bound both to Mn and Ca, a requirement imposed by MS experiments.[43] (ii) Similar timescales for the exchange in the S_2 state were found both for W_s in the MS (see ref. [26]) and for O5 in the EPR experiments. The later binding substrate water W_f has not yet been detected directly in experiments. However, recent EPR data indicate an OH^- to be bound to Mn_b in close vicinity to O5 in the S_3 state, consistent with DFT computations (Fig. 9).[29] It has recently been proposed that this OH^- as the second substrate is intro-

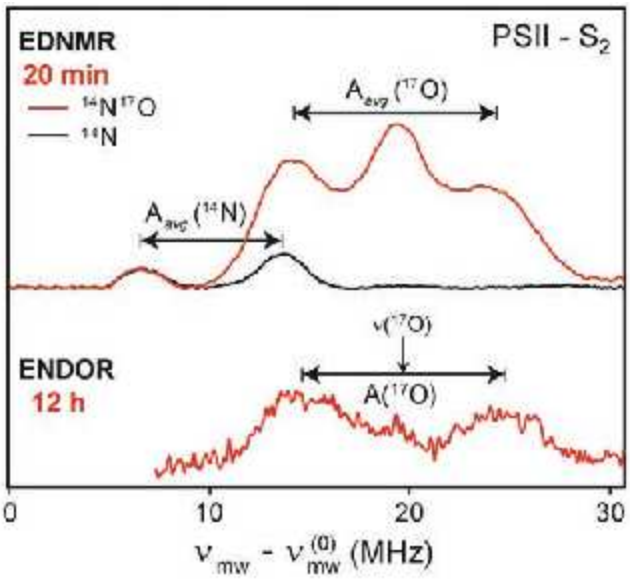

Fig. 7: W-band EDNMR of PS II in the S_2 state (top) compared to the corresponding ENDOR experiment (bottom). The sample buffer had been exchanged with $H_2{}^{17}O$ (90% enrichment) for 30 min (3x) in the dark prior to flash-advancement to the S_2 state (red traces). Similar experiments were also performed for the S_0 and the S_3 state (not shown). EDNMR spectra are also shown for $H_2{}^{16}O$ buffer (black trace), containing only ^{14}N signals (from histidine His332, see Fig. 2, top). The ^{17}O EDNMR signals were obtained in 20 min, whereas the respective ^{17}O ENDOR of the same sample took several hours.[40] Figure adapted from ref. [40].

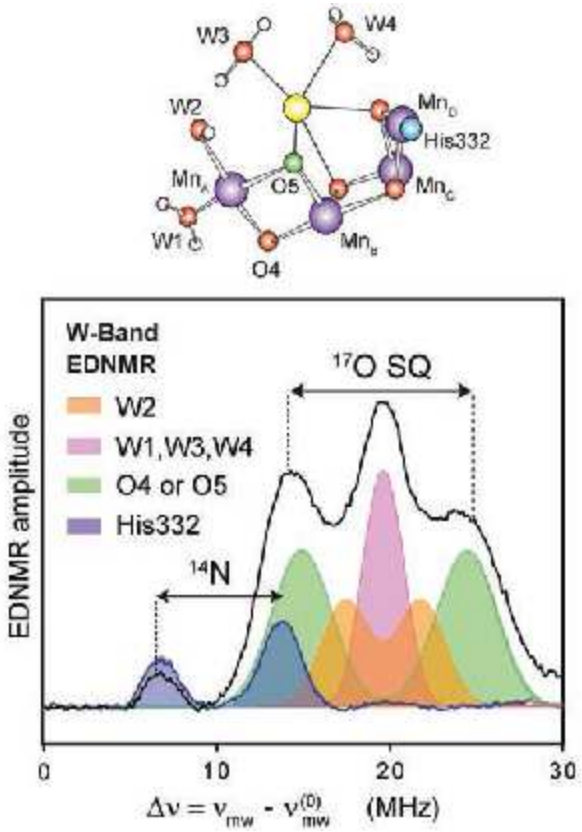

Fig. 8: Analysis of the ^{17}O EDNMR (single-quantum transitions) shown in Fig. 7. Three classes of oxygen ligands were assigned: the largest ^{17}O splitting belongs to the exchangeable μ-oxo bridge O5, the smaller ones to the H_2O/OH^- molecules as indicated. Several independent experiments identify the largest ^{17}O interaction to originate from O5.[40-43] On top, the Mn cluster is shown indicating μ-oxo bridges and bound H_2O/OH^- molecules. Figure adapted from ref. [40].

duced to this site by toggling between the open and closed cubane structures and is thus derived from W2, one of the terminal ligands of Mn_A (compare structure S_3 in Fig. 9). Other possibilities for the origin of W_f are Ca^{2+}-bound W3 or W4 or an additional water molecule binding to the cluster later than S_2.

As a consequence of the above results, only those mechanisms in which the O5 bridge represents the early binding substrate W_s come into consideration for the catalytic cycle of the enzymatic water oxidation reaction (Fig. 9, see refs. [8-9, 24]). W_s probably binds in the form of an OH^- in the S_0 state, being deprotonated completely during the subsequent oxidation step to S_1. In the S_3 state, the other substrate binding site at Mn_D is being occupied by an OH^- ligand. A further oxidation and deprotonation step leads to S_4. There are two possible scenarios with regards to the respective oxidation site: (i) the substrate W_f (ligand centered) or (ii) an Mn ion (metal centered). Thereby, a Mn^{IV}-oxyl or a Mn^{V}-oxo moiety, respectively, would be generated, and the O-O bond formation would either proceed as a radical coupling or via a nucleophilic attack. An oxo-oxyl coupling has already been proposed nearly ten years ago by Per Siegbahn (see ref. [44]). Further details of a catalytic cycle based on the latest findings are depicted in Fig. 9.

CONCLUSIONS FROM WATER OXIDATION IN PS II FOR AN EFFICIENT ARTIFICIAL PHOTOSYNTHESIS

The properties of the WOC in PS II described above represent valuable design features of bioinspired molecular catalysts for water oxidation. The following ones are considered essential for such catalysts:

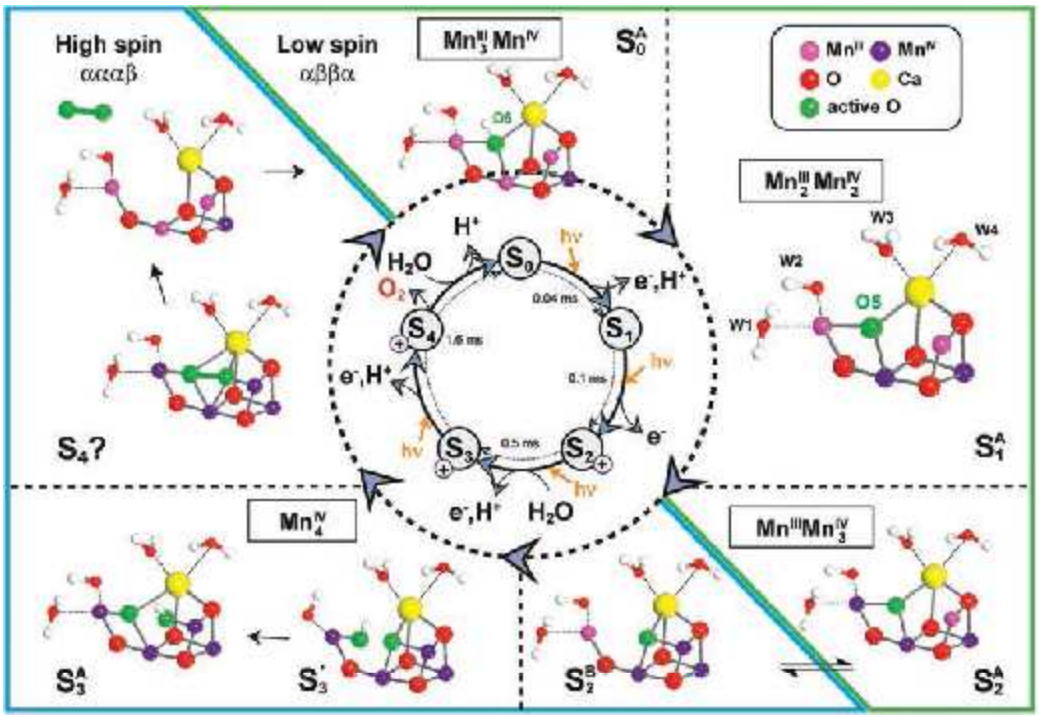

Fig. 9: Water splitting cycle based on spectroscopic and theoretical work (see refs. [8-9, 24]), detailing the structures of the Mn cluster in the different S states, the water binding events and the O-O bond formation and O_2 release. Switching of the preferred total spin state configuration of the cluster is thought to take place in S_2 from low to high spin and between S_4 and S_0 from high back to low spin, indicated by the diagonal line dividing the green and blue boxes. This may be necessary for the formation of triplet dioxygen $^3O_2$ in the final step of the cycle. Figure adapted from ref. [24].

1. The material of the catalyst must be abundant, easily accessible, inexpensive (i.e. no precious metals), non-toxic, sufficiently stable under working conditions and should thus be scalable.
2. The required four oxidizing equivalents must be stored in the catalyst to couple the fast 1-electron photochemical reaction with the slow 4-electron chemical water oxidation process.
3. The binding of the two substrate water molecules should take place at two well-defined neighboring metal centers, accompanied by their successive deprotonation and activation.
4. The redox steps of the catalytic metal centers should be of similar magnitude and in the range of 1 eV, and should finally lead to a concerted water oxidation, O_2 formation and release in order to avoid reactive oxygen intermediates. This requires sequential release of protons.
5. A functional matrix is needed mimicking the protein for efficient transport of water to the reaction site, release of oxygen and for proton management (as in PS II).
6. In the photochemical act, a light-induced species must be generated with sufficient oxidative potential to oxidize water (+0.82 V at pH 7).
7. Effective coupling of the charge separation with the catalytic center is necessary to diminish the overpotential (as via Y_Z in PS II).
8. The catalyst should be stable; in case of destruction, a mechanism of self-repair or healing should be in place to avoid deactivation of the catalyst.

At present, it is still a great challenge to create a catalyst that fulfills all the above criteria and could thus compete with the Mn cluster in PS II. The future will show if at least part of the points can be fulfilled. For examples of water splitting chemical catalysts see refs. [45-49].

ACKNOWLEDGEMENT

We thank all coworkers who contributed to this work (named in the respective references); in particular all theoretical work has been done in collaboration with Dimitrios Pantazis and Frank Neese in our institute. For financial support, the Max-Planck-Gesellschaft is gratefully acknowledged.

REFERENCES

[1] *BP Statistical Review of World Energy 2016,* http://www.bp.com/content/dam/bp/pdf/energy-economics/statistical-review-2016/bp-statistical-review-of-world-energy-2016-full-report.pdf,2 016.

[2] IPCC, *Climate Change 2014: Synthesis Report. Contribution of Working Groups I, II and III to the Fifth Assessment Report of the Intergovernmental Panel on Climate Change,* IPCC, Geneva, 2014.

[3] N. S. Lewis, D. G. Nocera, *Proc. Natl. Acad. Sci. U. S. A.* 2006, **103**,1 5729-15735.

[4] T. J. Wydrzynski, W. Hillier (Eds.), *Molecular Solar Fuels*, The Royal Society of Chemistry, Cambridge, 2011.

[5] R. Schlögl (Ed.), *Chemical Energy Storage*, De Gruyter, Berlin, 2012.

[6] S. A. Sherif, D. Y. Goswami, E. K. Stefanakos, A. Steinfeld, *Handbook of Hydrogen Energy*, CRC Press, Boca Raton, 2014.

[7] T. A. Faunce, W. Lubitz, A. W. Rutherford, D. R. MacFarlane, G. F. Moore, P. D. Yang, D. G. Nocera, T. A. Moore, D. H. Gregory, S. Fukuzumi, K. B. Yoon, F. A. Armstrong, M. R. Wasielewski, S. Styring, *Energy Environ. Sci.* 2013, **6**,6 95-698.

[8] N. Cox, W. Lubitz, *Green* 2013, **3**,2 35-263.

[9] N. Cox, D. A. Pantazis, F. Neese, W. Lubitz, *Interface Focus* 2015, **5**, 20150009 http://dx.doi.org/10.1098/rsfs.2015.0009.

[10] R. Croce, H. van Amerongen, *Nat. Chem. Biol.* 2014, **10**, 492-501.

[11] M. Calvin, *Science* 1962, **135**,8 79-889.

[12] M. Suga, F. Akita, K. Hirata, G. Ueno, H. Murakami, Y. Nakajima, T. Shimizu, K. Yamashita, M. Yamamoto, H. Ago, J. R. Shen, *Nature* 2015, **517**,9 9-103.

[13] Y. Umena, K. Kawakami, J.-R. Shen, N. Kamiya, *Nature* 2011, **473**,5 5-60.

[14] B. Kok, B. Forbush, M. McGloin, *Photochem. Photobiol.* 1970, **11**,4 57-475.

[15] M. Retegan, N. Cox, W. Lubitz, F. Neese, D. A. Pantazis, *Phys. Chem. Chem. Phys.* 2014, **16**,1 1901-11910.

[16] P. J. Nixon, F. Michoux, J. F. Yu, M. Boehm, J. Komenda, *Ann. Bot.* 2010, **106**,1 -16.

[17] T. Wydrzynski, S. Satoh (Eds.), *Photosystem II: The Light-Driven Water:Plastoquinone Oxidoreductase*, Springer, Dordrecht, 2005.

[18] A. Zouni, H. T. Witt, J. Kern, P. Fromme, N. Krauss, W. Saenger, P. Orth, *Nature* 2001, **409**,7 39-743.

[19] K. N. Ferreira, T. M. Iverson, K. Maghlaoui, J. Barber, S. Iwata, *Science* 2004, **303**,1 831-1838.

[20] A. Guskov, J. Kern, A. Gabdulkhakov, M. Broser, A. Zouni, W. Saenger, *Nat. Struct. Mol. Biol.* 2009, **16**,3 34-342.

[21] J. Yano, J. Kern, K. D. Irrgang, M. J. Latimer, U. Bergmann, P. Glatzel, Y. Pushkar, J. Biesiadka, B. Loll, K. Sauer, J. Messinger, A. Zouni, V. K. Yachandra, *Proc. Natl. Acad. Sci. U. S. A.* 2005, **102**,1 2047-12052.

[22] D. A. Pantazis, W. Ames, N. Cox, W. Lubitz, F. Neese, *Angew. Chem., Int. Ed.* 2012, **51**, 9935-9940.

[23] W. Ames, D. A. Pantazis, V. Krewald, N. Cox, J. Messinger, W. Lubitz, F. Neese, *J. Am. Chem. Soc.* 2011, **133**,1 9743-19757.

[24] V. Krewald, M. Retegan, F. Neese, W. Lubitz, D. A. Pantazis, N. Cox, *Inorg. Chem.* 2016, **55**,4 88-501.

[25] P. Joliot, G. Barbieri, R. Chabaud, *Photochem. Photobiol.* 1969, **10**,3 09-329.

[26] W. Hillier, T. Wydrzynski, *Coord. Chem. Rev.* 2008, **252**, 306-317.

[27] J. Messinger, G. Renger, in *Primary Processes of Photosynthesis, Part 2: Principles and Apparatus* (Ed.: G. Renger), 2008, The Royal Society of Chemistry, Cambridge, 2008; Vol. 9, pp. 291-349.

[28] T. Lohmiller, W. Ames, W. Lubitz, N. Cox, S. K. Misra, *Appl. Magn. Reson.* 2013, **44**,6 91-720.

[29] N. Cox, M. Retegan, F. Neese, D. A. Pantazis, A. Boussac, W. Lubitz, *Science* 2014, **345**,8 04-808.

[30] G. C. Dismukes, Y. Siderer, *Proc. Natl. Acad. Sci. U. S. A.* 1981, **78**,2 74-278.

[31] J. L. Casey, K. Sauer, *Biochim. Biophys. Acta, Bioenerg.* 1984, **767**,2 1-28.

[32] J. L. Zimmermann, A. W. Rutherford, *Biochim. Biophys. Acta, Bioenerg.* 1984, **767**,1 60-167.

[33] A. Boussac, J. J. Girerd, A. W. Rutherford, *Biochemistry* 1996, **35**,6 984-6989.

[34] A. Haddy, K. V. Lakshmi, G. W. Brudvig, H. A. Frank, *Biophys. J.* 2004, **87**,2 885-2896.

[35] L. V. Kulik, B. Epel, W. Lubitz, J. Messinger, *J. Am. Chem. Soc.* 2007, **129**,1 3421-13435.

[36] J. M. Peloquin, K. A. Campbell, D. W. Randall, M. A. Evanchik, V. L. Pecoraro, W. H. Armstrong, R. D. Britt, *J. Am. Chem. Soc.* 2000, **122**, 10926-10942.

[37] N. Cox, L. Rapatskiy, J.-H. Su, D. A. Pantazis, M. Sugiura, L. Kulik, P. Dorlet, A. W. Rutherford, F. Neese, A. Boussac, W. Lubitz, J. Messinger, *J. Am. Chem. Soc.* 2011, **133**,3 635-3648.

[38] V. Krewald, M. Retegan, N. Cox, J. Messinger, W. Lubitz, S. DeBeer, F. Neese, D. A. Pantazis, *Chem. Sci.* 2015, **6**,1 676-1695.

[39] T. Lohmiller, N. Cox, J. H. Su, J. Messinger, W. Lubitz, *J. Biol. Chem.* 2012, **287**,2 4721-24733.

[40] L. Rapatskiy, N. Cox, A. Savitsky, W. M. Ames, J. Sander, M. M. Nowaczyk, M. Rögner, A. Boussac, F. Neese, J. Messinger, W. Lubitz, *J. Am. Chem. Soc.* 2012, **134**,1 6619-16634.

[41] M. Pérez Navarro, W. M. Ames, H. Nilsson, T. Lohmiller, D. A. Pantazis, L. Rapatskiy, M. M. Nowaczyk, F. Neese, A. Boussac, J. Messinger, W. Lubitz, N. Cox, *Proc. Natl. Acad. Sci. U. S. A.* 2013, **110**,1 5561-15566.

[42] T. Lohmiller, V. Krewald, M. Pérez Navarro, M. Retegan, L. Rapatskiy, M. M. Nowaczyk, A. Boussac, F. Neese, W. Lubitz, D. A. Pantazis, N. Cox, *Phys. Chem. Chem. Phys.* 2014, **16**, 11877-11892.

[43] G. Hendry, T. Wydrzynski, *Biochemistry* 2003, **42**,6 209-6217.

[44] P. E. M. Siegbahn, *Acc. Chem. Res.* 2009, **42**,1 871-1880.

[45] M. W. Kanan, D. G. Nocera, *Science* 2008, **321**,1 072-1075.

[46] E. S. Andreiadis, M. Chavarot-Kerlidou, M. Fontecave, V. Artero, *Photochem. Photobiol.* 2011, **87**, 946-964.

[47] P. D. Tran, L. H. Wong, J. Barber, J. S. C. Loo, *Energy Environ. Sci.* 2012, **5**,5 902-5918.

[48] C. X. Zhang, C. H. Chen, H. X. Dong, J. R. Shen, H. Dau, J. Q. Zhao, *Science* 2015, **348**,6 90-693.

[49] P. Kurz, in *Solar Energy for Fuels* (Eds.: H. C. Tüysüz, Candace K.), Springer International Publishing, Switzerland, 2016, pp. 49-72.

INHALT HEFT 8 9 (2016)